Natural Product Sciences
19(2) : 127-136 (2013)

Hyperoside Protects Cells against Gamma Ray Radiation-Induced Apoptosis in Hamster Lung Fibroblast†

Mei Jing Piao[1], Ki Cheon Kim[1], Suk Ju Cho[1], Sungwook Chae[2], Sam Sik Kang[3], and Jin Won Hyun[1,*]

[1]*School of Medicine and Institute for Nuclear Science and Technology, Jeju National University, Jeju 690-756, Korea*
[2]*Aging Research Center, Korea Institute of Oriental Medicine, Daejeon 305-811, Korea*
[3] *Natural Products Research Institute and College of Pharmacy, Seoul National University, Seoul 110-460, Korea*

Abstract – Ionizing radiation, including that evoked by gamma (γ)-rays, induces oxidative stress through the generation of reactive oxygen species, resulting in apoptosis, or programmed cell death. This study aimed to elucidate the radioprotective effects of hyperoside (quercetin-3-O-galactoside) against γ-ray radiation-induced apoptosis in Chinese hamster lung fibroblasts, V79-4 and demonstrated that the compound reduced levels of intracellular reactive oxygen species in γ-ray-irradiated cells. Hyperoside also protected irradiated cells against DNA damage (evidenced by pronounced DNA tails and elevated phospho-histone H2AX and 8-oxoguanine content) and membrane lipid peroxidation. Furthermore, hyperoside prevented the γ-ray-provoked reduction in cell viability via the inhibition of apoptosis through the increased levels of Bcl-2, the decreased levels of Bax and cytosolic cytochrome c, and the decrease of the active caspase 9 and caspase 3 expression. Taken together, these results suggest that hyperoside defend cells against γ-ray radiation-induced apoptosis by inhibiting oxidative stress.
Keywords – Hyperoside (quercetin-3-O-galactoside), γ-Ray radiation, Apoptosis, Reactive oxygen species, Oxidative stress

Introduction

Ionizing radiation increases the production of reactive oxygen species (ROS), including superoxide anions, hydroxyl radicals, and hydrogen peroxide (H_2O_2), leading to oxidative stress and cell damage (Sies, 1983). ROS can oxidatively modify lipids, proteins, DNA, and small intracellular molecules. For example, the reaction of ROS with lipids generates lipid peroxides, leading to increased membrane permeability (Yang *et al*., 2007). Furthermore, the reaction of ROS with proteins gives rise to decreased protein synthesis due to ribosomal translocation and/or destruction of proteins, resulting in impaired cellular metabolism and accumulation of cellular waste products (Tuder *et al*., 2003). ROS can also cause damage to nucleic acids by altering purine and pyrimidine bases and by enhancing DNA strand breaks (Dizdaroglu *et al*., 2002).

Hyperoside (quercetin-3-O-galactoside), a flavonoid compound, possesses many defensive properties against ROS-induced damage, such as nitric oxide synthase inhibitory activity (Luo *et al*., 2004) and antioxidant activity (Zou *et al*., 2004). The compound also demonstrates antifungal activity (Li *et al*., 2005), antiviral activity (Chen *et al*., 2006; Wu *et al*., 2007), antidepressant activity (Prenner *et al*., 2007), and cardioprotective (Trumbeckaite *et al*., 2006) and neuroprotective effects (Liu *et al*., 2005). Recently, we reported that hyperoside decreases H_2O_2-induced cell damage through activation of an antioxidant system (Piao *et al*., 2008). However, little information is available regarding the protective capacity of hyperoside against cell damage stemming from gamma (γ)-ray radiation. Therefore, the present study investigated this question, as well as the mechanism of action of hyperoside against γ-ray-generated oxidative stress.

Experimental

Reagents – Hyperoside (quercetin-3-O-galactoside, Fig. 1) compound purified from aerial parts of *Metaplexis japonica* (Lee *et al*., 2012). 2', 7'-Dichlorodihydrofluorescein diacetate (DCF-DA), propidium iodide, and Hoechst 33342 were purchased from Sigma Chemical Company

†Dedicated to Prof. Sam Sik Kang of the Seoul National University for his leading works on Natural Products Research.
*Author for correspondence
School of Medicine and Institute for Nuclear Science and Technology, Jeju National University, Jeju 690-756, Korea
Tel: +82-64-754-3838; E-mail: jinwonh@jejunu.ac.kr

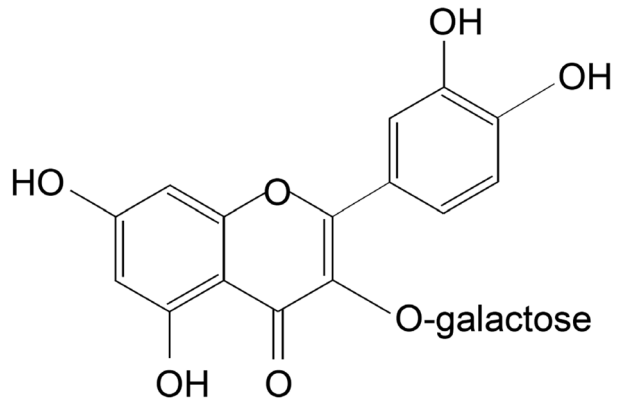

Fig. 1. Chemical structure of hyperoside (quercetin-3-O-galactoside).

(St. Louis, MO, USA). 5, 5', 6, 6'-Tetrachloro-1, 1', 3, 3'-tetraethylbenzimidazolylcarbocyanine iodide (JC-1) was purchased from the Invitrogen Corporation (Carlsbad, CA, USA), and diphenyl-1-pyrenylphosphine (DPPP) from Invitrogen (Poole, Dorset, UK). The primary anti-Bcl-2, -Bax, -cytochrome c, -caspase 9, -caspase 3 and -poly ADP-ribosyl polymerase (PARP) antibodies were purchased from Cell Signaling Technology (Beverly, MA, USA), and the primary anti-phospho H2A.X antibody from Upstate Biotechnology (Lake Placid, NY, USA).

Cell culture and irradiation – Chinese hamster lung fibroblast (V79-4) cells from the American Type Culture Collection (Rockville, MD, USA) were maintained at 37 °C in an incubator with a humidified atmosphere of 5% CO_2 and cultured in Dulbecco's modified Eagle's medium, containing 10% heat-inactivated fetal calf serum, streptomycin (100 μg/ml) and penicillin (100 units/ml). The cells were exposed to γ-ray irradation at 1.5 Gy/min from a ^{60}Co γ-ray source (MDS Nordion C-188 standard source, Jeju National University, Jeju, Korea).

Intracellular reactive oxygen species (ROS) measurement – Cells were treated with hyperoside at 5 μM and were exposed to γ-ray radiation an hour later. The cells were incubated for an additional 24 h at 37 °C. After adding 25 μM of DCF-DA solution, the fluorescence of 2', 7'-dichlorofluorescein was detected using a Perkin Elmer LS-5B spectrofluorometer and a flow cytometer (Becton Dickinson, Mountain View, CA, USA), respectively (Rosenkranz *et al*., 1992). The image analysis for the generation of intracellular ROS was achieved by seeding the cells on a cover-slip loaded six well plate at 2×10^5 cells/well. Sixteen hours after plating, the cells were treated with hyperoside at 5 μM. An hour following hyperoside treatment and then irradiated with 10 Gy of γ-ray. Twenty four hours later, 100 μM of DCF-DA was added to each well and was incubated for an additional 30 min at 37 °C. After washing with phosphate-buffered saline (PBS), the stained cells were mounted onto a microscope slide in mounting medium (DAKO, Carpinteria, CA, USA). The microscopic images were collected using the Laser Scanning Microscope 5 PASCAL program (Carl Zeiss, Jena, Germany) on a confocal microscope.

Single cell gel electrophoresis (Comet assay) – A comet assay was performed to determine the degree of oxidative DNA damage (Rajagopalan *et al*., 2003). The cell suspension was mixed with 75 μl of 0.5% low melting agarose (LMA) at 39 °C, and spread on a fully frosted microscopic slide pre-coated with 200 μl of 1% normal melting agarose (NMA). After the solidification of the agarose, the slide was covered with another 75 μl of 0.5% LMA and then immersed in a lysis solution (2.5 M NaCl, 100 mM Na-EDTA, 10 mM Tris, 1% Trion X-100, and 10% DMSO, pH 10) for 1 h at 4 °C. The slides were then placed in a gel-electrophoresis apparatus containing 300 mM NaOH and 10 mM Na-EDTA (pH 13) for 40 min to allow for DNA unwinding and the expression of the alkali labile damage. Next, an electrical field was applied (300 mA, 25 V) for 20 min at 4 °C to draw the negatively charged DNA toward an anode. After the electrophoresis, the slides were washed three times for 5 min at 4 °C in a neutralizing buffer (0.4 M Tris, pH 7.5), followed by staining with 75 μl of propidium iodide (20 μg/ml). The slides were observed with a fluorescence microscope and image analyzer (Kinetic Imaging, Komet 5.5, UK). The percentage of the total fluorescence in the tail and the tail length of the 50 cells per slide were recorded.

Western blot analysis – Cells were treated with hyperoside at 5 μM and with γ-ray radiation at 10 Gy, an hour later. Next, the cells were incubated for 48 h at 37 °C, and harvested, followed by washing twice with PBS. The harvested cells were then lysed on ice for 30 min in 100 μl of a lysis buffer [120 mM NaCl, 40 mM Tris (pH 8), 0.1% NP 40] and centrifuged at 13,000 × g for 15 min. The supernatants were collected from the lysates and the protein concentrations were determined. Aliquots of the lysates (40 μg of protein) were boiled for 5 min and electrophoresed in 10% SDS-polyacrylamide gel. The blots in the gels were transferred onto nitrocellulose membranes (Bio-Rad, Hercules, CA, USA), and subsequently incubated with anti-primary antibodies. The membranes were further incubated with secondary anti-immunoglobulin-G-horseradish peroxidase conjugates (Pierce, Rockford, IL, USA), followed by exposure to X-ray film. The protein bands were detected using an

enhanced chemiluminescence western blotting detection kit (Amersham, Little Chalfont, Buckinghamshire, UK).

8-Oxoguanine (8-OxoG) level determination – Cellular DNA was isolated using the DNAzol reagent (Life Technologies, Grand Island, NY, USA) and quantified using a spectrophotometer. The quantity of 8-oxoG in DNA was determined using a Bioxytech 8-OHdG (8-hydroxy-2'-deoxyguanosine, a nucleoside of 8-oxoG)-ELISA kit purchased from OXIS Health Products (Portland, OR, USA) following the manufacturer's instructions.

Lipid peroxidation assay – Lipid peroxidation was estimated using the fluorescent probe DPPP as described by Okimoto *et al*. (2000). The image analysis for the lipid peroxidation was achieved by seeding the cells on a cover-slip loaded four well glass slide at 2×10^5 cells/well. The cells were treated with hyperoside at 5 μM. An hour following hyperoside treatment, the plate was irradiated with 10 Gy of γ-ray. Forty eight hours later, 5 μM of DPPP was added to each well and was incubated for an additional 15 min in the dark. After washing with PBS, the stained cells were mounted onto a microscope slide in mounting medium (DAKO, Carpinteria, CA, USA). The microscopic images were collected using the Laser Scanning Microscope 5 PASCAL program (Carl Zeiss, Jena, Germany) on a confocal microscope. The capture images of DPPP fluorescence by reactive species in the fluorescence DAPI region (excitation, 351 nm; emission, 380 nm).

Cell viability – The effect of hyperoside on the cell viability was determined using the [3-(4, 5-dimethylthiazol-2-yl)-2, 5-diphenyltetrazolium] bromide (MTT) assay, which is based on the reduction of a tetrazolium salt by mitochondrial dehydrogenase in viable cells (Carmichael *et al*., 1987). Cells were treated with hyperoside at 5 μM and with γ-ray. Forty eight hours later, 50 μl of the MTT stock solution (2 mg/ml) was added to each well to reach a total reaction volume of 200 μl. After incubating for 4 h, the plate was centrifuged at 800 × g for 5 min followed by aspiration of the supernatants. The formazan crystals in each well were dissolved in 150 μl of dimethyl sulfoxide and the A_{540} was read on a scanning multi-well spectrophotometer.

Nuclear staining with Hoechst 33342 – Cells were treated with hyperoside at 5 μM and with γ-ray radiation at 10 Gy an hour later. Next, the cells were incubated for an additional 48 h at 37 ºC. 1.5 μl of Hoechst 33342 (stock 10 mg/ml), which is a DNA-specific fluorescent dye, was added to each well and incubated for 10 min at 37 ºC. The stained cells were visualized under a fluorescent microscope, equipped with a CoolSNAP-Pro color digital camera to examine the degree of nuclear condensation.

Detection of apoptotic sub-G_1 hypodiploid cells – The amount of apoptotic sub-G_1 hypodiploid cells was determined using flow cytometer (Nicoletti *et al*., 1991). Cells were treated with hyperoside at 5 μM and with γ-ray radiation at 10 Gy, an hour later. Next, the cells were incubated for an additional 48 h at 37 ºC, followed by harvesting and fixing in 1 ml of 70% ethanol for 30 min at 4 ºC. The cells were then washed twice with PBS, and incubated for 30 min in the dark at 37 ºC in 1 ml of PBS containing 100 μg of propidium iodide and 100 μg of RNase A. A flow cytometric analysis was performed using a FACS Calibur flow cytometer. The sub-G_1 hypodiploid cells were assessed based on the histograms generated by the Cell Quest and Mod-Fit computer programs.

DNA fragmentation – Cells were treated with hyperoside at 5 μM and with γ-ray radiation at 10 Gy, an hour later. Cellular DNA fragmentation was assessed by analyzing the cytoplasmic histone-associated DNA fragmentation, using a kit from Roche Diagnostics (Portland, OR, USA) according to the manufacturer's instructions.

Mitochondrial membrane potential ($\Delta\psi_m$) analysis – Cells were treated with hyperoside at 5 μM and with γ-ray radiation at 10 Gy, an hour later. Cells were harvested, washed and suspended in PBS containing JC-1 (10 μg/ml). After 15 min of incubation at 37 ºC, the cells were washed, suspended in PBS and analyzed by flow cytometer (Troiano *et al*., 2007).

Statistical analysis – All measurements were made in triplicate and all values were expressed as the means ± standard error of the mean. The results were subjected to an analysis of variance (ANOVA) using the Tukey test to analyze the difference. $P < 0.05$ were considered significantly.

Results and Discussion

Flavonoids are increasingly being recognized as powerful antioxidants, with a potential role in chemoprevention in human cells (Afaq and Mukhtar 2006; Zhang *et al*., 2006; Ferguson, 2001; Nijveldt *et al*., 2001; Middleton *et al*., 2000). Flavonoids directly neutralize free radicals, chelate metal ions responsible for catalyzing lipid peroxidation, and induce the expression and/or activity of antioxidant enzymes (e.g., superoxide dismutase and glutathione peroxidase) (Nijveldt *et al*., 2001). Hyperoside (Fig. 1) is a flavonoid (Zou *et al*., 2004) that protects cells against H_2O_2-induced damage via the

activation of cellular antioxidants (Piao *et al*., 2008). Therefore, the current study explored the ability of hyperoside to safeguard cells against ionizing radiation.

Exposure of cells to ionizing radiation (cosmic rays, α-particles, β-particles, X-rays, and γ-rays) causes damage to lipids, proteins, and DNA through the production of ROS, followed by the induction of oxidative stress (Lin *et al*., 2003). Of particular interest to the current study, irradiation with γ-rays triggers a diverse array of functional changes in cells due to the interaction of γ-ray-generated ROS with multiple cellular organelles. Indeed, considerable evidence demonstrates that ROS play an important role in the destructive actions of γ-ray radiation (Bhosle *et al*., 2005; Choi *et al*., 2007).

Recently we reported that the intracellular ROS scavenging activity of hyperoside in V79-4 cells after H_2O_2 treatment was 30% at 1 μM, 70% at 2.5 μM, and 84% at 5 μM, however, there was not clear difference of ROS scavenging effect at 5, 25, 50, and 100 μM of hyperoside (Piao *et al*., 2008). Therefore, we determined to choose 5 μM as an optimal dose of hyperoside for further study of γ-ray radiation.

In the current study, the free radical scavenging effect of hyperoside on γ-ray-induced ROS was first explored. Spectrofluorometric analysis indicated that ROS levels assessed by staining with DCF-DA were significantly higher in irradiated (10 Gy) cells than in control or only hyperoside-treated cells, whereas hyperoside (5 μM)-pretreatment in irradiated cells decreased ROS levels (Fig. 2A). This pattern was confirmed by flow cytometry, revealing a fluorescence intensity value of 349 in hyperoside-pretreated, irradiated cells, compared with a

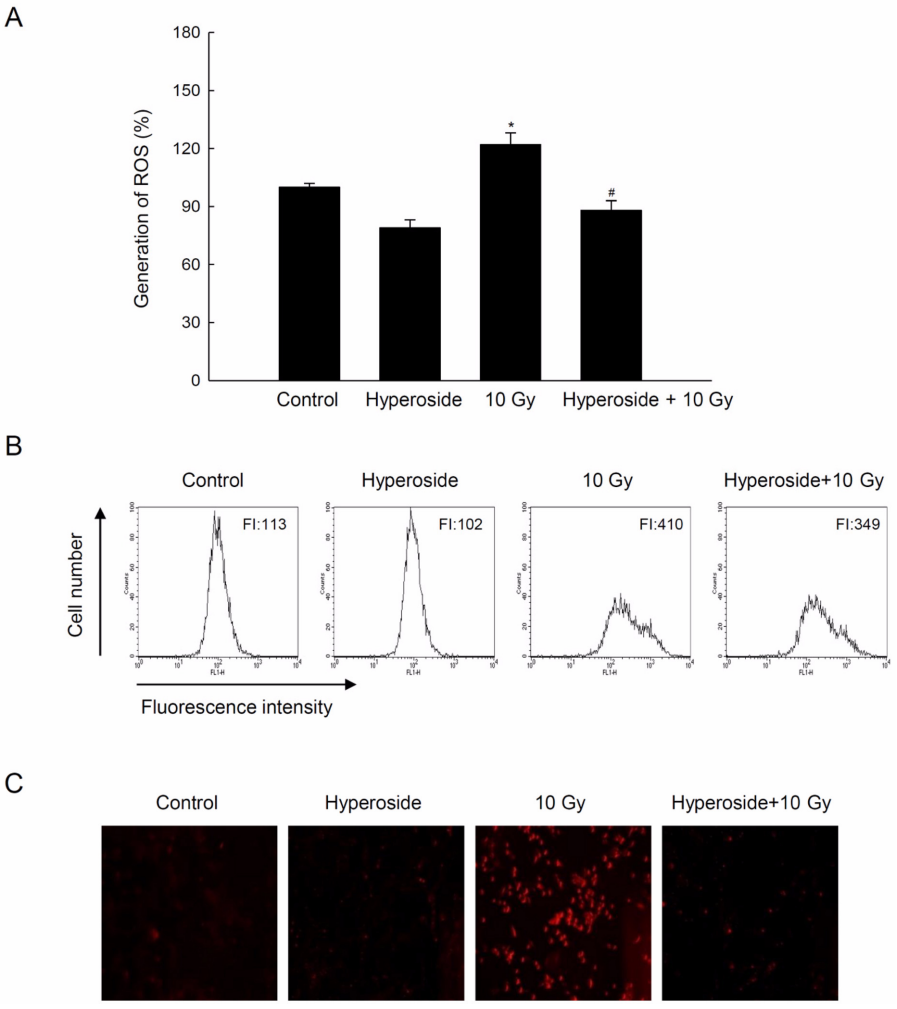

Fig. 2. Hyperoside scavenges intracellular ROS generated by γ-ray radiation. Cells were treated with hyperoside (5 μM), followed by γ-ray irradiation (10 Gy) 1 h later, and were incubated for a further 24 h. Intracellular ROS were then detected by (A) fluorescence spectrophotometry, (B) flow cytometry, and (C) confocal microscopy after DCF-DA staining. *Indicates significantly different from untreated control cells ($p < 0.05$), and $^{\#}$indicates significantly different from irradiated cells ($p < 0.05$).

value of 410 in irradiated cells (Fig. 2B). Furthermore, confocal microscopy indicated that the red fluorescence intensity of DCF-DA-stained ROS was also higher in irradiated cells than in untreated control and hyperoside-treated cells (Fig. 2C). On the other hand, hyperoside treatment 1 h prior to γ-ray exposure reduced the fluorescence intensity in the irradiated cells. These findings suggest that hyperoside can scavenge ROS generated by γ-ray radiation.

Radiation-induced ROS attack vital cellular biomolecules and organelles, generally leading to lethal cell damage. DNA and cell membranes are the two key targets of radiation-induced cell lethality. Thus, the ability of hyperoside to inhibit cellular DNA damage and

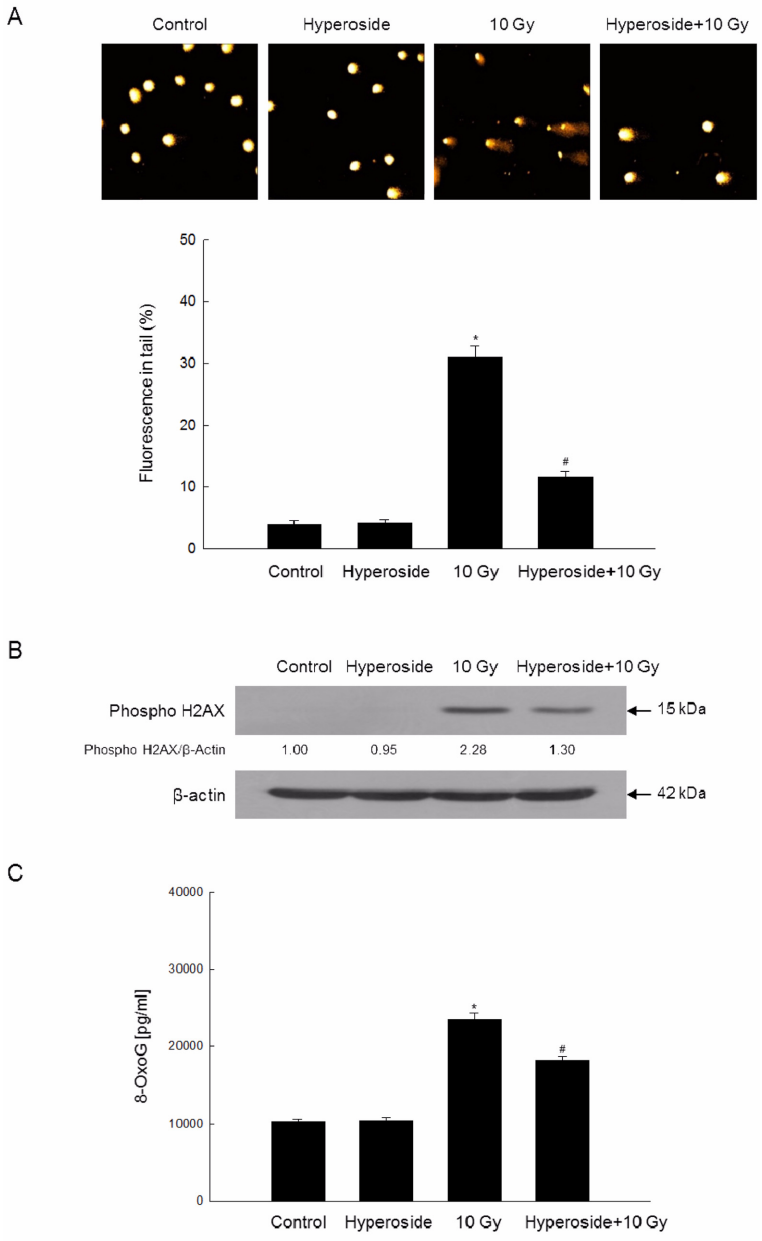

Fig. 3. Hyperoside mitigates γ-ray radiation-induced cellular DNA damage. Cells were pretreated with hyperoside (5 μM), followed by γ-ray irradiation (10 Gy) 1 h later, and were incubated for a further 48 h. (A) Representative images and the percentage of cellular DNA in the comet tails were detected by an alkaline comet assay. *Indicates significantly different from untreated control cells ($p < 0.05$), and #indicates significantly different from irradiated cells ($p < 0.05$). (B) Cell lysates were collected and subjected to Western blotting analysis. The phospho-histone H2AX protein was detected using a specific antibody. β-actin was employed as a loading control. (C) The 8-oxoG content in cellular DNA was measured using an ELISA kit. *Indicates significantly different from untreated control cells ($p < 0.05$), and #indicates significantly different from irradiated cells ($p < 0.05$).

membrane lipid peroxidation was next investigated in γ-ray-irradiated cells. DNA damage was detected by using an alkaline comet assay, by assessing phospho-histone H2AX expression, and by measuring the amount of 8-oxoG in untreated control, hyperoside-treated, irradiated, and hyperoside-pretreated, irradiated cells. The comet assay demonstrated that exposure of cells to γ-ray radiation increased the parameters of DNA tail length (microscopic images in Fig. 3A) and the percentage of DNA in the tails. The percentage of DNA in the tails increased from about 4% in control cells to 31% in irradiated cells, whereas pretreatment with hyperoside resulted in a decrease to 12% (Fig. 3A).

The phosphorylation of nuclear histone H2AX, a sensitive marker for breaks in double-stranded DNA (Bonner *et al*., 2008), was then assessed by Western blotting. H2AX phosphorylation was higher in irradiated cells than in untreated control and only hyperoside-treated cells (Fig. 3B). However, hyperoside pretreatment decreased the expression of phospho-H2AX in irradiated cells. Finally, 8-oxoG adducts in damaged DNA have been extensively used as biomarkers of oxidative stress (Tope and Panemangalore, 2007). The γ-ray radiation increased the 8-oxoG content to 23481 pg/ml (228%) compared to 10298 pg/ml (100%) in untreated control cells, while hyperoside decreased the 8-oxoG content in irradiated cells to 18251 pg/ml (177%) (Fig. 3C). This observation is indicative of a protective effect of hyperoside against γ-ray-induced DNA damage. Flavonoids can promote an increase in the expression of several DNA repair genes in various biological systems (Bouhlel *et al*., 2008; Gao *et al*., 2006; Jagetia *et al*., 2007; Guarrera *et al*., 2007). These reports indicate that hyperoside is likely involved in the repair of γ-ray-evoked DNA damage via the induction of DNA repair-related regulators. In addition to DNA damage, γ-ray radiation causes damage to cell membranes. Cell membrane lesions are in large part responsible for the loss of cell viability following exposure to ionizing radiation. Fig. 4 demonstrated that lipid peroxidation, as monitored using the fluorescent probe DPPP, was greater in cells exposed to γ-ray radiation than in untreated control and only hyperoside-treated cells. Conversely, hyperoside prevented γ-ray irradiation-induced peroxidation of lipids. These inhibitory effects of hyperoside against lipid and DNA damage probably contributed to cytoprotection against radiation-induced cell death.

In many cases, γ-ray radiation-induced cell death occurs via apoptotic events (Kim *et al*., 2007; Lee *et al*., 2007). Therefore, the ability of hyperoside to promote cell survival in γ-ray-irradiated cells was next evaluated. Cell survival was reduced from ~100% in untreated control and hyperoside-treated cells to 66% in irradiated cells (Fig. 5A). However, pretreatment with hyperoside increased cell survival to 79%. To evaluate a cytoprotective effect of hyperoside via the inhibition of apoptosis stimulated by γ-ray radiation, cell nuclei were next stained with Hoechst 33342. The fluorescence microscopic images in Fig. 5B demonstrate that untreated control and only hyperoside-treated cells had intact nuclei, while the irradiated cells showed significant nuclear fragmentation, which is characteristic of apoptosis. On the other hand, treatment of cells with hyperoside for 1 h prior to irradiation yielded a dramatic decrease in nuclear fragmentation.

The protective effect of hyperoside against apoptosis was also confirmed by analysis of the apoptotic sub-G_1 DNA content, by ELISA-based quantification of cytoplasmic histone-associated DNA fragmentation, and by investigation of the mitochondrial membrane potential ($\Delta\psi_m$). The analysis of the apoptotic sub-G_1 DNA content revealed an increase from 2% in untreated and only hyperoside-treated cells to 27% in irradiated cells (Fig. 5C). By contrast, treatment with hyperoside decreased the apoptotic sub-G_1 DNA content to 17%. The irradiated cells had

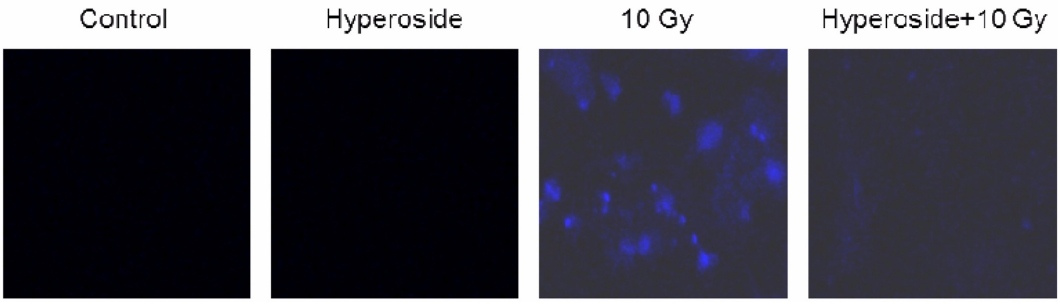

Fig. 4. Hyperoside safeguards cells against γ-ray irradiation-induced lipid peroxidation. Cells were treated with hyperoside (5 μM), followed by γ-ray irradiation (10 Gy) 1 h later, and were incubated for a further 48 h. Lipid peroxidation was measured by quantifying DPPP fluorescence.

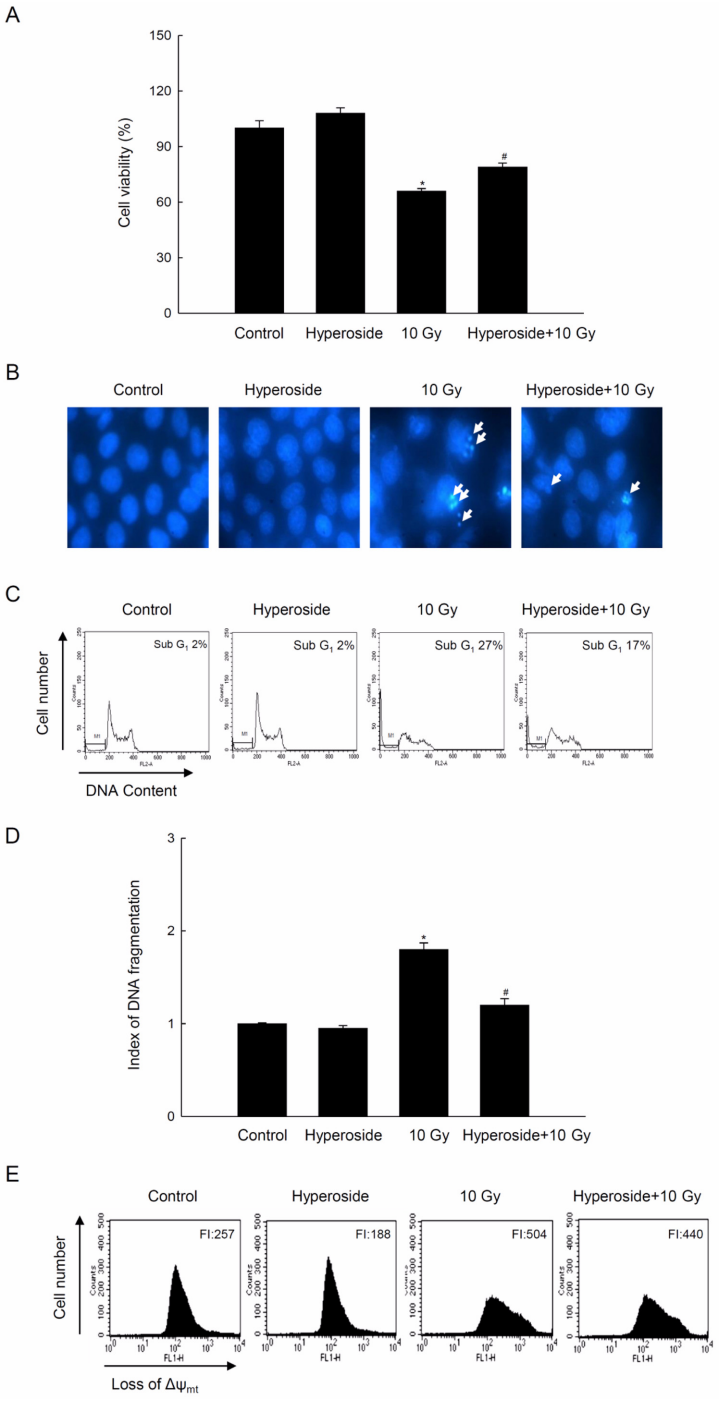

Fig. 5. Hyperoside reduces γ-ray irradiation-induced apoptosis. Cells were treated with hyperoside (5 μM), followed by γ-ray irradiation (10 Gy) 1 h later, and incubated for a further 48 h. (A) Cell viability was determined by employing the MTT assay. *Indicates significantly different from untreated control cells ($p < 0.05$), and #indicates significantly different from irradiated cells ($p < 0.05$). (B) Apoptotic body formation was observed under a fluorescence microscope after Hoechst 33342 staining. Apoptotic bodies are indicated by arrows. (C) The apoptotic sub-G_1 DNA content was detected by flow cytometry after propidium iodide staining. (D) DNA fragmentation was quantified by using an ELISA kit. *Indicates significantly different from untreated control cells ($p < 0.05$), and #indicates significantly different from irradiated cells ($p < 0.05$). (E) The mitochondrial membrane potential ($\Delta\psi_m$) was analyzed by flow cytometry after staining cells with JC-1. FI, fluorescence intensity.

higher levels of cytoplasmic histone-associated DNA fragmentation than the control groups; however, treatment with hyperoside significantly decreased the level of DNA fragmentation (Fig. 5D).

The apoptotic process is characterized by the opening of mitochondrial membrane pores (Landes *et al*., 2011), bringing about the loss of $\Delta\psi_m$. To investigate changes in $\Delta\psi_m$, cells were stained with the fluorescent dye JC-1. Notably, exposure of cells to γ-ray radiation resulted in the loss of $\Delta\psi_m$, as observed by an increase in JC-1 fluorescence (Fig. 5E). Consistent with its other anti-apoptotic actions, hyperoside partially blocked the increase in mitochondrial membrane permeability and the loss of $\Delta\psi_m$.

To elucidate the protective mechanism of action of hyperoside in terms of γ-ray irradiation-induced cell death, changes in the expression levels of Bcl-2 (B-cell lymphoma 2), an anti-apoptotic protein, and Bax (Bcl-2-associated X protein), a pro-apoptotic protein, were examined. Bcl-2 expression was significantly lower and Bax expression was significantly higher in irradiated cells than in untreated control or only hyperoside-treated cells (Fig. 6). Cytosolic cytochrome c levels were also higher in irradiated cells than in control cells. These changes were alleviated by hyperoside pretreatment. Importantly, Bcl-2 prevents the opening of the mitochondrial membrane pore during the apoptotic process, while Bax promotes its opening (Renault *et al*., 2013). As discussed above, the pore opening induces the loss of $\Delta\psi_m$, which in turn stimulates the release of cytochrome c from the mitochondria into the cytosol (Liu and Luo, 2012; Renault *et al*., 2013). As such, we suggest that the ability of hyperoside to block the loss of $\Delta\psi_m$ in irradiated cells (Fig. 5E) results from the up-regulation of Bcl-2 and the down-regulation of Bax, which inhibits the release of mitochondrial cytochrome c.

We next examined caspase 9 expression by Western blotting analysis, because this pro-apoptotic enzyme is activated by mitochondrial membrane disruption (Perkins *et al*., 2000). Cells exposed to γ-ray radiation had increased levels of the active form of caspase 9 (35 kDa) and caspase 3 (19 kDa). These cells also had increased levels of cleaved (inactivated) poly ADP ribose polymerase (PARP, 89 kDa), which is significant as PARP is inactivated by activated caspases. However, hyperoside inhibited γ-ray radiation-induced activation of caspase 9 and caspase 3 and the subsequent cleavage of PARP. However, there is a report regarding the prooxidant activity of flavonoids were related with concentration. For example, prooxidant properties of quercetin, naringenin, hesperetin, and morin were evaluated according to different concentrations in human lymphocytes (Yen *et al*., 2003). Concentration range is important criteria between antioxidant and prooxidant. In this paper, hyperoside at 5 μM showed antioxidant activity and the maximum concentrations for working as antioxidant properties are remained for further study.

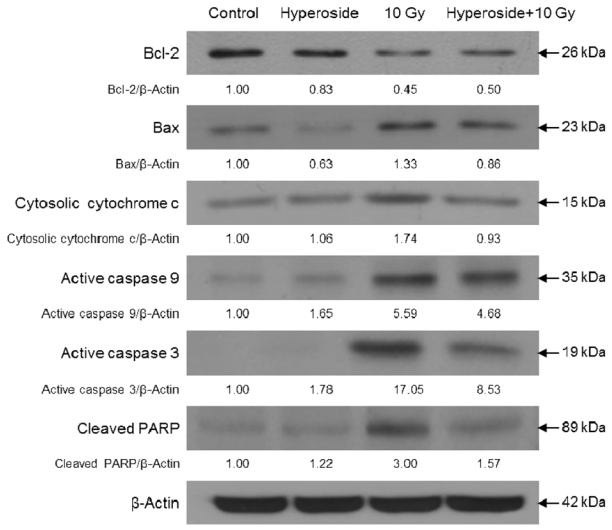

Fig. 6. Hyperoside modulates the expression of apoptosis regulatory proteins. Cells were treated with hyperoside (5 μM), followed by γ-ray irradiation (10 Gy) 1 h later, and were incubated for a further 48 h. Cell lysates were collected and subjected to Western blotting analysis. Bcl-2, Bax, cytosolic cytochrome c, active caspase 9, active caspase 3, and cleaved PARP proteins were detected by using specific antibodies. β-actin was employed as a loading control.

Taken together, the results of the present study suggest that hyperoside exerts cytoprotective actions against γ-ray radiation-induced apoptosis via ROS scavenging. Furthermore, hyperoside inhibits mitochondrial membrane disruption resulting from γ-ray exposure, and the downstream activation of caspases. Based on our results, it suggests that hyperoside may be possibly useful as a radioprotective compound.

Acknowledgement

This study was supported by a grant from the National R&D Program for Cancer Control, Ministry for Health and Welfare, Korea (1120340).

References

Afaq, F. and Mukhtar, H., Botanical antioxidants in the prevention of photocarcinogenesis and photoaging. *Exp. Dermatol.* **15**, 678-684 (2006).

Bhosle, S.M., Huilgol, N.G., and Mishra, K.P., Enhancement of radiation-induced oxidative stress and cytotoxicity in tumor cells by ellagic acid. *Clin. Chim. Acta* **359**, 89-100 (2005).

Bouhlel, I., Valenti, K., Kilani, S., Skandrani, I., Ben Sghaier, M., Mariotte, A.M., Dijoux-Franca, M.G., Ghedira, K., Hininger-Favier, I., Laporte, F., and Chekir-Ghedira, L., Antimutagenic, antigenotoxic and

antioxidant activities of *Acacia salicina* extracts (ASE) and modulation of cell gene expression by H_2O_2 and ASE treatment. *Toxicol. In Vitro* **22**, 1264-1272 (2008).

Bonner, W.M., Redon, C.E., Dickey, J.S., Nakamura, A.J., Sedelnikova, O.A., Solier, S., and Pommier, Y., Gamma H2AX and cancer. *Nat. Rev. Cancer* **8**, 957-967 (2008).

Carmichael, J., DeGraff, W.G., Gazdar, A.F., Minna, J.D., and Mitchell, J.B., Evaluation of a tetrazolium-based semiautomated colorimetric assay: assessment of chemosensitivity testing. *Cancer Res.* **47**, 936-941 (1987).

Chen, L., Li, J., Luo, C., Liu, H., Xu, W., Chen, G., Liew, O. W., Zhu, W., Puah, C. M., Shen, X., and Jiang, H., Binding interaction of quercetin-3-beta-galactoside and its synthetic derivatives with SARS-CoV 3CL(pro): structure-activity relationship studies reveal salient pharmacophore features. *Bioorg. Med. Chem.* **14**, 8295-8306 (2006).

Choi, K.M., Kang, C.M., Cho, E.S., Kang, S.M., Lee, S.B., and Um, H.D., Ionizing radiationinduced micronucleus formation is mediated by reactive oxygen species that are produced in a manner dependent on mitochondria, Nox1, and JNK. *Oncol. Rep.* **17**, 1183-1188 (2007).

Dizdaroglu, M., Jaruga, P., Birincioglu, M., and Rodriguez, H., Free radical-induced damage to DNA: mechanisms and measurement. *Free Radic. Biol. Med*. **32**, 1102-1115 (2002).

Ferguson, L.R., Role of plant polyphenols in genomic stability. *Mutat. Res.* **475**, 89-111 (2001).

Gao, K., Henning, S.M., Niu, Y., Youssefian, A.A., Seeram, N.P., Xu, A., and Heber, D., The citrus flavonoid naringenin stimulates DNA repair in prostate cancer cells. *J. Nutr. Biochem.* 17, 89-95 (2006).

Guarrera, S., Sacerdote, C., Fiorini, L., Marsala, R., Polidoro, S., Gamberini, S., Saletta, F., Malaveille, C., Talaska, G., Vineis, P., and Matullo, G., Expression of DNA repair and metabolic genes in response to a flavonoid-rich diet. *Br. J. Nutr.* 98, 525-533 (2007).

Jagetia, A., Jagetia, G.C., and Jha, S., Naringin, a grapefruit flavanone, protects V79 cells against the bleomycin-induced genotoxicity and decline in survival. *J. Appl. Toxicol.* 27, 122-132 (2007).

Kim, S.Y., Seo, M., Oh, J.M., Cho, E.A., and Juhnn, Y.S., Inhibition of gamma ray-induced apoptosis by stimulatory heterotrimeric GTP binding protein involves Bcl-xL downregulation in SH-SY5Y human neuroblastoma cells. *Exp. Mol. Med.* **39**, 583-593 (2007).

Landes, T., and Martinou, J.C., Mitochondrial outer membrane permeabilization during apoptosis: the role of mitochondrial fission. *Biochim. Biophys. Acta* **1813**, 540-545 (2011).

Lee, J.H., Kim, S.Y., Kil, I.S., and Park, J.W., Regulation of ionizing radiation-induced apoptosis by mitochondrial NADP+-dependent isocitrate dehydrogenase. *J. Biol. Chem.* **282**, 13385-13394 (2007).

Lee, S.Y., Kim, J.S., and Kang, S.S., Flavonol glycosides from the aerial parts of *Metaplexis japonica*. *Kor. J. Pharmacogn*. **43**, 206-212 (2012).

Li, S., Zhang, Z., Cain, A., Wang, B., Long, M., and Taylor, J., Antifungal activity of camptothecin, trifolin, and hyperoside isolated from *Camptotheca acuminata*. *J. Agric. Food Chem.* **53**, 32-37 (2005).

Lin, X., Zhang, F., Bradbury, C.M., Kaushal, A., Li, L., Spitz, D.R., Aft, R.L., and Gius, D., 2-Deoxy-D-glucose-induced cytotoxicity and radiosensitization in tumor cells is mediated via disruptions in thiol metabolism. *Cancer Res.* **63**, 3413-3417 (2003).

Liu, Y. and Luo, W., Betulinic acid induces Bax/Bak-independent cytochrome c release in human nasopharyngeal carcinoma cells. *Mol. Cells* **33**, 517-524 (2012).

Liu, Z., Tao, X., Zhang, C., Lu, Y., and Wei, D., Protective effects of hyperoside (quercetin-3-o-galactoside) to PC12 cells against cytotoxicity induced by hydrogen peroxide and tert-butyl hydroperoxide. *Biomed. Pharmacother*. **59**, 481-490 (2005).

Luo, L., Sun, Q., Mao, Y.Y., Lu, Y.H., and Tan, R.X., Inhibitory effects of flavonoids from *Hypericum perforatum* on nitric oxide synthase. *J. Ethnopharmacol.* **93**, 221-225 (2004).

Middleton, E.Jr., Kandaswami, C., and Theoharides, T.C., The effects of plant flavonoids on mammalian cells: implications for inflammation, heart disease, and cancer. *Pharmacol. Rev.* **52**, 673-751 (2000).

Nicoletti, I., Migliorati, G., Pagliacci, M.C., Grignani, F., and Riccardi, C., A rapid and simple method for measuring thymocyte apoptosis by propidium iodide staining and flow cytometry. *J. Immunol. Methods* **139**, 271-279 (1991).

Nijveldt, R.J., van Nood, E., van Hoorn, D.E., Boelens, P.G., van Norren, K., and van Leeuwen, P.A., Flavonoids: a review of probable mechanisms of action and potential applications. *Am. J. Clin. Nutr.* **74**, 418-425 (2001).

Okimoto, Y., Watanabe, A., Niki, E., Yamashita, T., and Noguchi, N., A novel fluorescent probe diphenyl-1-pyrenylphosphine to follow lipid peroxidation in cell membranes. *FEBS Lett.* **474**, 137-140 (2000).

Perkins, C.L., Fang, G., Kim, C.N., and Bhalla, K.N., The role of Apaf-1, caspase-9, and bid proteins in etoposide- or paclitaxel-induced mitochondrial events during apoptosis. *Cancer Res.* **60**, 1645-1653 (2000).

Piao, M.J., Kang, K.A., Zhang, R., Ko, D.O., Wang, Z.H., You, H.J., Kim, H.S., Kim, J.S., Kang, S.S., and Hyun, J.W., Hyperoside prevents oxidative damage induced by hydrogen peroxide in lung fibroblast cells via an antioxidant effect. *Biochim. Biophys. Acta* **1780**, 1448-1457 (2008).

Prenner, L., Sieben, A., Zeller, K., Weiser, D., and Haberlein, H., Reduction of High-Affinity beta(2)-Adrenergic Receptor Binding by Hyperforin and Hyperoside on Rat C6 Glioblastoma Cells Measured by Fluorescence Correlation Spectroscopy. *Biochemistry* **46**, 5106-5113 (2007).

Rajagopalan, R., Ranjan, S.K., and Nair, C.K., Effect of vinblastine sulfate on gammaradiation-induced DNA single-strand breaks in murine tissues. *Mutat. Res.* **536**, 15-25 (2003).

Renault, T.T., Teijido, O., Antonsson, B., Dejean, L.M., and Manon, S., Regulation of Bax mitochondrial localization by Bcl-2 and Bcl-x(L): keep your friends close but your enemies closer. *Int. J. Biochem. Cell Biol*. **45**, 64-67 (2013).

Rosenkranz, A.R., Schmaldienst, S., Stuhlmeier, K.M., Chen,W., Knapp,W., and Zlabinger, G.J., A microplate assay for the detection of oxidative products using 2',7'-dichlorofluorescein-diacetate. *J. Immunol. Methods* **156**, 39-45 (1992).

Sies, H., *Oxidative Stress*, Academic Press, New York, 1983.

Tope, A.M. and Panemangalore, M., Assessment of oxidative stress due to exposure to pesticides in plasma and urine of traditional limited-resource farm workers: formation of the DNA-adduct 8-hydroxy-2-deoxy-guanosine (8-OHdG). *J. Environ. Sci. Health B* **42**, 151-155 (2007).

Troiano, L., Ferraresi, R., Lugli, E., Nemes, E., Roat, E., Nasi,M., Pinti, M., and Cossarizza, A., Multiparametric analysis of cells with different mitochondrial membrane potential during apoptosis by polychromatic flow cytometry. *Nat. Protoc.* **2**, 2719-2727 (2007).

Trumbeckaite, S., Bernatoniene, J., Majiene, D., Jakstas, V., Savickas, A., and Toleikis, A., The effect of flavonoids on rat heart mitochondrial function. *Biomed. Pharmacother.* **60**, 245-248 (2006).

Tuder, R.M., Zhen, L., and Cho, C.Y., Taraseviciene-Stewart, L., Kasahara, Y., Salvemini, D., Voelkel, N.F., and Flores, S.C., Oxidative stress and apoptosis interact and cause emphysema due to vascular endothelial growth factor receptor blockade. *Am. J. Respir. Cell. Mol. Biol.* **29**, 88-97 (2003).

Wu, L.L., Yang, X.B., Huang, Z.M., Liu, H.Z., and Wu, G.X., In vivo and in vitro antiviral activity of hyperoside extracted from *Abelmoschus manihot* (L) medik. *Acta. Pharmacol. Sin.* **28**, 404-409 (2007).

Yang, P., He, X.Q., Peng, L., Li, A.P., Wang, X.R., Zhou, J.W., and Liu, Q.Z., The role of oxidative stress in hormesis induced by sodium

arsenite in human embryo lung fibroblast (HELF) cellular proliferation model. *J. Toxicol. Environ. Health A* **70**, 976-983 (2007).
Yen, G.C., Duh, P.D., Tsai, H.L., and Huang, S.L., Pro-oxidative properties of flavonoids in human lymphocytes. Bioscience, *Biotech. Biochem*. **67**, 1215-1222 (2003).
Zhang, J., Stanley, R.A., Adaim, A., Melton, L.D., and Skinner, M.A., Free radical scavenging and cytoprotective activities of phenolic antioxidants. *Mol. Nutr. Food Res.* **50**, 996-1005 (2006).
Zou, Y., Lu, Y., and Wei, D., Antioxidant activity of a flavonoid-rich extract of *Hypericum perforatum L. in vitro*. *J. Agric. Food Chem.* **52**, 5032-5039 (2004).

Received March 27, 2013
Revised May 24, 2013
Accepted June 2, 2013